# Stability analysis for periodic solutions of the Van der Pol–Duffing forced oscillator



2016 Phys. Scr. 91 015201

(http://iopscience.iop.org/1402-4896/91/1/015201)

IOP Publishing | Royal Swedish Academy of Sciences Physica Scripta
Phys. Scr. 91 (2016) 015201 (7pp) doi:10.1088/0031-8949/91/1/015201

# Stability analysis for periodic solutions of the Van der Pol–Duffing forced oscillator

**Jifeng Cui, Jiaming Liang and Zhiliang Lin**

State Key Laboratory of Ocean Engineering School of Naval Architecture, Ocean and Civil Engineering Shanghai Jiao Tong University, Shanghai 200240, People's Republic of China

E-mail: linzhiliang@sjtu.edu.cn

Received 9 July 2015, revised 3 October 2015
Accepted for publication 5 November 2015
Published 2 December 2015

**Abstract**

Based on the homotopy analysis method (HAM), the high accuracy frequency response curve and the stable/unstable periodic solutions of the Van der Pol-Duffing forced oscillator with the variation of the forced frequency are obtained and studied. The stability of the periodic solutions obtained is analyzed by use of Floquet theory. Furthermore, the results are validated in the light of spectral analysis and bifurcation theory.

Keywords: periodicity, stability, HAM, floquet theory

(Some figures may appear in colour only in the online journal)

## 1. Introduction

Basically, all the problems encountered in all areas of sciences and engineering are nonlinear from the outset. Nonlinear equations are always used to describe complex systems and nonlinear phenomena. Therefore, how to solve these equations has become an important and tough problem, because their solutions are valuable for the understanding of nonlinear interaction and behaviors of complex system. Frequently, analytical and numerical methods are used to investigate nonlinear problems. In general, it is often more costly to get an analytic approximation than a numerical one to a given nonlinear problem [1].

In this paper, we consider the Van der Pol-Duffing forced oscillator governed by the equation

$$\ddot{x} - \mu\left(1 - x^2\right)\dot{x} + \Omega_0^2 x + \alpha x^3 = F\cos(\Omega t), \tag{1}$$

which was first explored and reported by Ueda [2]. In equation (1), $x$ denotes displacement from the equilibrium position, the dot denotes the derivative of $x$ with respect to $t$, $\mu > 0$ is the damping parameter, $\Omega$ and $F$ are the frequency and amplitude of the external force, respectively, and $\Omega_0$ and $\alpha$ are constants.

Obviously, when $\mu = 0$, equation (1) becomes the Duffing equation. The Duffing equation was investigated by the German inventor and engineer Georg Duffing when he was working on vibrations. He examined the effects of quadratic and cubic stiffness nonlinearities, and completed his 134 page monograph with the title 'Forced oscillations with variable natural frequency and their technical significance' [3]. Conversely, when $\alpha = 0$, equation (1) is the Van der Pol equation. The Van der Pol oscillator was originally proposed by the Dutch electrical engineer and physicist Balthasar van der Pol while he was studying electrical circuits. The Van der Pol equation has a long history of being used in both the physical and biological sciences [4, 5]. A number of analytical and numerical methods have been used to investigate both of them [6]. Thus, equation (1) is essentially equivalent to a combination of Van der Pol and Duffing oscillators and has widespread applications in the modelling of nonlinear oscillation processes. For example, equation (1) is used to model optical bistability in a dispersive medium, in which the refractive index is dependent on the optical intensity [7]. Besides, Ghorbanian *et al* propose a novel phenomenological model of the EEG signal based on the dynamics of a coupled Van der Pol–Duffing oscillator network, and some interesting phenomena has been observed [8]. Murali and Lakshmanan investigate the phenomena of chaos synchronization and efficient signal transmission in a physically interesting model named the Van der Pol-Duffing oscillator [9]. Moreover, the system (1) was considered from a mathematical point-of-view by the authors in reference [10], and the study was confined to the region of driving frequency which is close to and below the principal resonance (principal resonance occurs when $\Omega$ is close to the frequency of the limit cycle of the unforced system of equation (1) with $F = 0$). It is worth mentioning that in 1994 the occurrence of chaotic motion in the forced Van der Pol–Duffing oscillator in close neighbourhood of the principal resonance was considered and interpreted in connection with subcritical Neimark bifurcation by Szempliriska-Stupnicka and Rudowski [11]. In 1997, Venkatesan and Lakshmanan showed that the double-well Van der Pol–Duffing oscillator with the parameter choice $|\alpha| = \beta$ exhibited a rich variety of attractors of periodic, quasiperiodic, and chaotic types by numerical studies [12]. In 2011, Chudzik *et al* discussed the mechanism leading to the multistability in the externally excited Van der Pol–Duffing oscillator [13], etc. The rich nonlinear properties including limit cycle, quasi-periodic motion, bifurcation routes, chaotic dynamics and jump phenomena are also given in [14–16].

Due to considering the periodic solution, the transformation

$$\tau = \Omega t, \quad u(\tau) = x(t), \tag{2}$$

is introduced. Then, equation (1) becomes

$$\Omega^2\ddot{u} - \mu\Omega\left(1 - u^2\right)\dot{u} + \Omega_0^2 u + \alpha u^3 = F\cos\tau. \tag{3}$$

The purpose of this paper is to obtain the high accuracy approximate stable/unstable periodic solutions of equation (1) analytically. Then, the stability of the periodic solutions obtained with specific sets of parameters are analyzed by use of Floquet theory. The results agree with those of spectral analysis and bifurcation theory.

## 2. Homotopy analysis method

In this section, an analytic approximate method named the homotopy analysis method (HAM) [17, 18] is employed to obtain the stable/unstable periodic solutions of equation (3). This approach has been widely used in solving a variety of nonlinear systems [19–28]. Here, we only outline the main procedures.

Note that equation (3) could represent a periodic motion with period of $2\pi$. Therefore $u(\tau)$ can be expressed by a set of base functions such as

$$\{\cos(m\tau), \sin(m\tau)|m = 0, 1, 2, 3, ...\}. \tag{4}$$

That is

$$u(\tau) = \sum_{m=0}^{\infty}\left(\alpha_m\cos(m\tau) + \beta_m\sin(m\tau)\right), \tag{5}$$

where $\alpha_m$, $\beta_m$ are constant coefficients.

The HAM provides us great freedom in choosing auxiliary linear operators and initial guess solutions [18]. Based on the type of the governing equation and the solution expression (5), the auxiliary linear operator is chosen as

$$\mathcal{L}f = \frac{\partial^2 f}{\partial\tau^2} + f. \tag{6}$$

Note that the operator $\mathcal{L}$ has the property

$$\mathcal{L}\left(C_1\cos\tau + C_2\sin\tau\right) = 0, \tag{7}$$

for any constant coefficients $C_1$ and $C_2$.

Considering the rule of solution expression (5) and the property of $\mathcal{L}$, the initial guess solution can be chosen as

$$u_0(\tau) = a_0\sin\tau + b_0\cos\tau, \tag{8}$$

where $a_0$ and $b_0$ are unknowns to be determined.

According to equation (3), a nonlinear operator is defined as

$$\mathcal{N}f = \Omega^2\ddot{f} - \Omega\mu\left(1 - f^2\right)\dot{f} + \Omega_0^2 f + \alpha f^3 - F\cos\tau. \tag{9}$$

The so-called zeroth-order deformation equation is constructed as

$$(1 - q)\mathcal{L}\left[\Phi(\tau; q) - u_0(\tau)\right] = q\, c_0\mathcal{N}[\Phi(\tau; q)], \tag{10}$$

where $c_0$ is the non-zero convergence-control parameter and $q$ is an embedding parameter.

When $q = 0$, equation (10) has the solution

$$\Phi(\tau; 0) = u_0(\tau). \tag{11}$$

When $q = 1$, equation (10) is the same as equation (3), provided

$$\Phi(\tau; 1) = u(\tau). \tag{12}$$

Thus, as the embedding parameter $q$ increases from 0 to 1, the solution $\Phi(\tau; q)$ of the zeroth-order deformation equation deforms from the initial guess $u_0(\tau)$ to the exact solution $u(\tau)$.

From Taylor's theorem, $\Phi(\tau; q)$ is expanded as a power series in $q$ as follows

$$\Phi(\tau; q) = u_0(\tau) + \sum_{n=1}^{\infty}u_n(\tau)q^n, \tag{13}$$

where

$$u_n(\tau) = \frac{1}{n!}\frac{\partial^n\Phi(\tau; q)}{\partial q^n}\bigg|_{q=0}. \tag{14}$$

Assume the value of $c_0$ is properly chosen so that equation (13) is convergent at $q = 1$. Then, due to equation (12), one has

$$u(\tau) = u_0(\tau) + \sum_{n=1}^{\infty}u_n(\tau), \tag{15}$$

For simplicity, the vector is defined as

$$\mathbf{u}_k = \{u_0, u_1, u_2, \ldots, u_k\}. \tag{16}$$

Differentiating the zeroth-order deformation equation (10) $m$ times with respect to $q$, then dividing by $m!$ and finally setting $q = 0$, the so-called $m$th-order deformation equation is obtained as

$$\mathcal{L}\left[u_m(\tau) - \chi_m u_{m-1}(\tau)\right] = c_0 R_m(\tau), \tag{17}$$

where

$$R_m = \frac{1}{(m-1)!} \frac{\partial^{m-1} \mathcal{N}[\Phi(\tau;q)]}{\partial q^{m-1}}\bigg|_{q=0}$$
$$= \Omega^2 \ddot{u}_{m-1} - \Omega\mu\dot{u}_{m-1} + \Omega\mu \sum_{i=0}^{m-1} \dot{u}_i \sum_{j=0}^{m-1-i} u_j u_{m-1-i-j} + \Omega_0^2 u_{m-1} + \alpha \sum_{i=0}^{m-1} u_i \sum_{j=0}^{m-1-i} u_j u_{m-1-i-j} - (1-\chi_m)F\cos\tau, \quad (18)$$

and

$$\chi_m = \begin{cases} 0, & m \leqslant 1, \\ 1, & m > 1. \end{cases} \quad (19)$$

For the $m$th-order deformation equation (17), the term on the right hand side $R_m$ is given. Considering the rule of the solution expression (5) and the definition of the operator $\mathcal{L}$, i.e. equation (6), the $R_m$ also can be expressed by

$$R_m = a_{m,1}\sin\tau + b_{m,1}\cos\tau + \sum_{\substack{i=0\\ i\neq 1}}^{M} a_{m,i}\sin(i\tau) + \sum_{\substack{j=0\\ j\neq 1}}^{M} b_{m,j}\sin(j\tau), \quad (20)$$

where, $a_{m,i}, b_{m,j}$ $(i, j = 0, 1, 2, \ldots, M)$ are constant coefficients, and $M$ is the number of items. According to the property (7), if $a_{m,1} \neq 0$ and $b_{m,1} \neq 0$, then $u_m(\tau)$ contains the so-called secular terms $\tau\cos(\tau)$ and $\tau\sin(\tau)$, which are not periodic. This kind of secular terms must be avoided. Therefore,

$$a_{m,1} = 0, \quad b_{m,1} = 0, \quad (21)$$

are enforced. For the present problem, when $m = 1$, it is found that $a_0$ and $b_0$ satisfy the subsequent system of nonlinear equations

$$\begin{cases} \left(\Omega_0^2 - \Omega^2\right)a_0 + \frac{3}{4}\alpha a_0^3 + \mu\Omega b_0 - \frac{1}{4}\mu\Omega a_0^2 b_0 + \frac{3}{4}\alpha a_0 b_0^2 - \frac{1}{4}\mu\Omega b_0^3 = 0 \\ -F - \mu\Omega a_0 + \frac{1}{4}\mu\Omega a_0^3 + \left(\Omega_0^2 - \Omega^2\right)b_0 + \frac{3}{4}\alpha a_0^2 b_0 + \frac{1}{4}\mu\Omega a_0 b_0^2 + \frac{3}{4}\alpha b_0^3 = 0 \end{cases} \quad (22)$$

So, $a_0$ and $b_0$ can be determined by solving the system of equations (22), that is, $u_0(\tau)$ is now known. Similarly, $u_1(\tau)$, $u_2(\tau)$, … can be obtained sequentially. At this point, the solution of the $m$th-order deformation equation (17) is obtained as

$$u_m = \chi_m u_{m-1} + \bar{a}_{m,1}\sin\tau + \bar{b}_{m,1}\cos\tau + \sum_{\substack{i=0\\ i\neq 1}}^{M} \bar{a}_{m,i}\sin(i\tau) + \sum_{\substack{j=0\\ j\neq 1}}^{M} \bar{b}_{m,j}\sin(j\tau), \quad (23)$$

where

$$\bar{a}_{m,i} = \frac{a_{m,i}}{1-i^2}, \quad (i = 0, 2, 3, \ldots, M), \quad (24)$$

$$\bar{b}_{m,j} = \frac{b_{m,j}}{1-j^2}, \quad (j = 0, 2, 3, \ldots, M). \quad (25)$$

However, the two unknowns $\bar{a}_{m,1}$ and $\bar{b}_{m,1}$ can be obtained by the two additional equations (21) from the $m+1$ th-order deformation equation, and they are always governed by a series of linear equations ($m \geqslant 1$). Obviously, using a symbolic algebra system such as Mathematica 9.0, $\bar{a}_{m,i}$, $\bar{b}_{m,j}$, $u_m$, $(i = j = 0, 2, 3, \ldots, M;\ m = 0, 1, 2, \ldots, M)$ can be obtained successively.

Eventually, we obtain the results at the $K$th-order approximation as

$$U_K(\tau) \approx \sum_{m=1}^{K} u_m(\tau), \quad (26)$$

and $A = \max\{|x(t)|, t \in [0, T]\}$ is defined to analyze the amplitude response.

In order to choose a proper value of $c_0$, the squared residual error is defined

$$\mathcal{E}_K(c_0) = \int_0^{2\pi} \left(\mathcal{N}\left[U_K(\tau)\right]\right)^2 d\tau. \quad (27)$$

For the sake of computational efficiency, the squared residual error $\mathcal{E}_K(c_0)$ is calculated numerically, i.e.

$$\mathcal{E}_K(c_0) \approx E_K(c_0) = \frac{1}{N+1}\sum_{k=0}^{N} \left(\mathcal{N}\left[U_K(\tau)\right]\big|_{\tau=k\Delta\tau}\right)^2, \quad (28)$$

where $\Delta\tau = 2\pi/N$ and $N$ is an integer. $N = 50$ is set in this paper. Note that $E_K(c_0)$ depends on the convergence-control parameter $c_0$. Obviously, the smaller the value of $E_K(c_0)$ for given $K$, the better the approximation. At the given order of approximation $K$, the optimal approximation is defined by the minimum of $E_K(c_0^*)$ with the corresponding optimal convergence-control parameter $c_0^*$.

## 3. Results and discussion

Without loss of generality, a set of parameters $\mu = \frac{1}{10}$, $\Omega_0 = \alpha = F = 1$, $\Omega = 2$ is considered. From equation (22), three families of solutions are obtained, as shown in table 1. To illustrate the convergence of the HAM series solutions, take Solution C ($a_0 = 0.142962$, $b_0 = 2.14443$) for example. As shown in figure 1, as the order of the approximation increases, the discrete squared residual $E_K(c_0)$ decreases in the region

**Table 1.** The solutions of system in the case of $\mu = \frac{1}{10}$, $\Omega_0 = \alpha = F = 1$, $\Omega = 2$.

| Solutions of system | $a_0$ | $b_0$ |
|---|---|---|
| Solution A | −0.120169 | -1.80254 |
| Solution B | −0.0227929 | -0.341894 |
| Solution C | 0.142962 | 2.14443 |

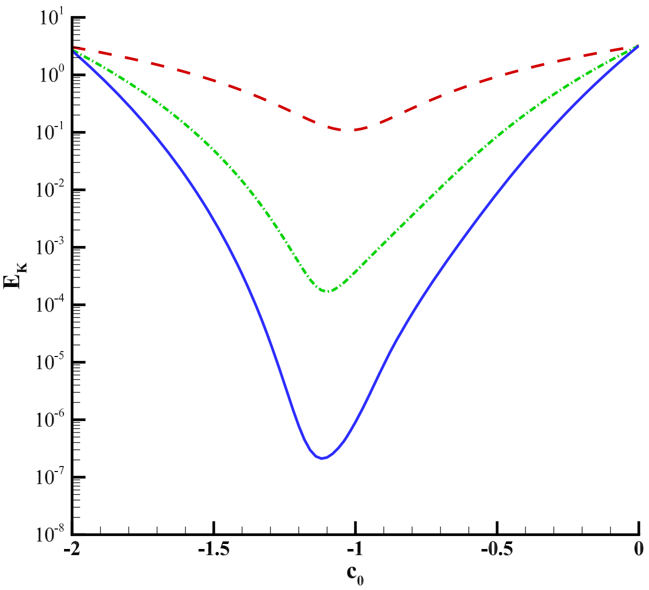


**Figure 1.** The discrete squared residual $E_K(c_0)$ of Solution C in the case of $\mu = \frac{1}{10}$, $\Omega_0 = \alpha = F = 1$, $\Omega = 2$. Dashed line: first-order approx.; dash-dot line: third-order approx.; solid line: fifth-order approx.

$\boldsymbol{R}_c = \{c_0| - 1.5 \leqslant c_0 \leqslant 0.5\}$. When $\frac{dE_5}{c_0} = 0$, the optimal convergence-control parameter $c_0$ is chosen as $c_0 = -\frac{11}{10}$. Similarly, the optimal convergence-control parameters $c_0$ of Solution A and Solution B can be properly chosen as $c_0 = -1$ and $c_0 = -\frac{9}{10}$, respectively. It is found that, as the order of the approximation increases, the discrete squared residuals of all these homotopy-series decrease monotonously. All HAM series solutions are expanded to the 20th order with residual error less than $5 \times 10^{-29}$, as shown in table 2. Also, the three families of analytic approximations of $u(t)$ compared with numerical results based on a fourth-order Runge Kutta method are plotted in figure 2. It is worth noting that the numerical results obtained by the fourth-order Runge Kutta method only agree closely with the series for Solution C. This means that, using HAM, we can obtain analytically the other two sets of periodic solutions which cannot be found by numerical methods.

To study the above interesting phenomenon, the stability of the periodic solutions is summarized in the context of Floquet theory, and the details of stability analysis are stated in the appendix. The criterion for stability is the maximum modulus of the calculated eigenvalues $\lambda_1$, $\lambda_2$ of the periodic solutions. If $|\lambda_i| < 1 (i = 1, 2)$, the periodic solution is stable, otherwise it is unstable. As shown in table 3, in the case of $\mu = \frac{1}{10}$, $\Omega_0 = \alpha = F = 1$, $\Omega = 2$, both eigenvalues of the periodic solution C are less than 1, but at least one eigenvalue of the periodic Solutions A ($\lambda_1 = 2.74895$, $\lambda_2 = 0.302832$) and Solution B ($\lambda_1 = \lambda_2 = 1.15935$) is greater than 1. Thus according to the Floquet theory, we can draw the conclusion that Solution C is stable and the other two are unstable with this set of parameters. This is the reason why we cannot obtain the numerical results which can agree with Solution A and Solution B.

Based on the HAM series solutions, the high accuracy frequency-response curve is shown in figure 3. In figure 3, we can see that there are multiple solutions when $1.647 \leqslant \Omega \leqslant 2.62$, and there is only one solution when $0.7 \leqslant \Omega < 1.647$ and $2.62 < \Omega \leqslant 4$. Through analyzing the residual errors (28) and frequency spectrums based on the fast Fourier transform (FFT) point by point, and using the stability analysis, we reach the conclusion that branch *b–c–d* (branch *b–c–d* is composed of two different branches $b-c$ and $c-d$, and $b-c$ does not belong to the multiple solutions domain $1.647 \leqslant \Omega \leqslant 2.62$) of the harmonic solution and is periodic and stable; branch *d–e–f* is periodic but unstable (branch *d–e–f* is composed of two different branches $d-e$ and $e-f$; they all belong to the multiple solutions domain $1.647 \leqslant \Omega \leqslant 2.35$). The remaining branches $a-b$ and *f–g–h* (branch *f–g–h* is composed of two different branches $f-g$ and $g-h$, and branch $f-g$ belongs to the multiple solutions domain $1.647 \leqslant \Omega \leqslant 2.62$) give strong indications that one may expect almost-periodic or chaotic solutions to occur in the domain. In other words, the two branches $a-b$ and *f–g–h* are so unstable that the periodic solutions may transit into almost-periodic or chaotic solutions with a very small initial perturbation. This result agrees with the analytic conclusions obtained by the use of topological methods [29]. For example, in the case of $\Omega_3 = 1.37$, one of the two characteristic frequencies is the forcing frequency $\Omega\,(0.2179 \times 2\pi = 1.36911)$, and the other is approximately equal to $3\Omega\,(0.6531 \times 2\pi = 4.10355)$, as shown in the schematic spectrum diagram figure 4. However, in the case of $\Omega = 1.36$, which is a little smaller than $\Omega_3$, in addition to the forced frequency $\Omega\,(0.21633 \times 2\pi = 1.35924)$ is found, the rest of the frequencies are so complex that we cannot even discover the inherent relations among them, as shown in figure 5. It is important to note that the above spectral analyses are based on the numerical simulations obtained by the fourth-order Runge Kutta method in the time domain $t \in [99900, 100000]$, which guarantees that the steady calculations are chosen. It illustrates that the HAM series solution is stable in the case of $\Omega_3 = 1.37$ and is unstable in the case of $\Omega = 1.36$. Based on the Floquet theory, $\lambda_1 = \lambda_2 = 0.997474$ ($\Omega_3 = 1.37$) and $\lambda_1 = \lambda_2 = 1.00077$ ($\Omega = 1.36$) are obtained, respectively, which agrees well with the conclusion above. The same conclusion was reached based on bifurcation theory. That is, in the region of

**Table 2.** The discrete square residual $E_K(c_0)$ of the three families of solutions in the case of $\mu = \frac{1}{10}$, $\Omega_0 = \alpha = F = 1$, $\Omega = 2$.

| | Solution A | Solution B | Solution C |
|---|---|---|---|
| $K$ | $E_K(c_0 = -1)$ | $E_K\left(c_0 = -\frac{9}{10}\right)$ | $E_K\left(c_0 = -\frac{11}{10}\right)$ |
| 1 | $1.41912 \times 10^{-2}$ | $3.60553 \times 10^{-8}$ | $1.25086 \times 10^{-1}$ |
| 5 | $8.89597 \times 10^{-10}$ | $6.64199 \times 10^{-19}$ | $2.20587 \times 10^{-7}$ |
| 10 | $7.05235 \times 10^{-19}$ | $3.47279 \times 10^{-30}$ | $1.43247 \times 10^{-14}$ |
| 15 | $6.52819 \times 10^{-28}$ | $2.37431 \times 10^{-41}$ | $7.81488 \times 10^{-22}$ |
| 20 | $6.65395 \times 10^{-37}$ | $2.89802 \times 10^{-52}$ | $3.93288 \times 10^{-29}$ |

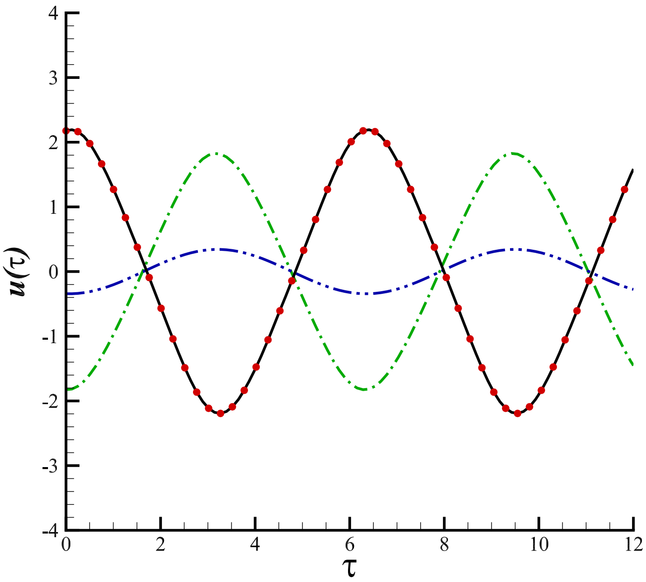


**Figure 2.** The system of solutions in the case of $\mu = \frac{1}{10}$, $\Omega_0 = \alpha = F = 1$, $\Omega = 2$. Dash-dot line: Solution A approx. ($c_0 = -1$); dash-dot-dot line: Solution B approx. ($c_0 = -\frac{9}{10}$); solid line: Solution C approx. ($c_0 = -\frac{11}{10}$); filled circle: numerical results.

**Table 3.** The eigenvalues in the case of $\mu = \frac{1}{10}$, $\Omega_0 = \alpha = F = 1$, $\Omega = 2$ by use of Floquet theory.

| | $\lvert\lambda_1\rvert$ | $\lvert\lambda_2\rvert$ |
|---|---|---|
| Solution A | 2.74895 | 0.302832 |
| Solution B | 1.15935 | 1.15935 |
| Solution C | 0.82505 | 0.82505 |

$1.37 \leqslant \Omega \leqslant 2.35$, there exist stable periodic solutions in the case of $\mu = \frac{1}{10}$, $\Omega_0 = \alpha = F = 1$, as shown in figure 6.

## 4. Concluding remarks

The stability of the periodic HAM series solutions of the Van der Pol-Duffing forced oscillator is studied in this paper. Some conclusions can be drawn as follows.

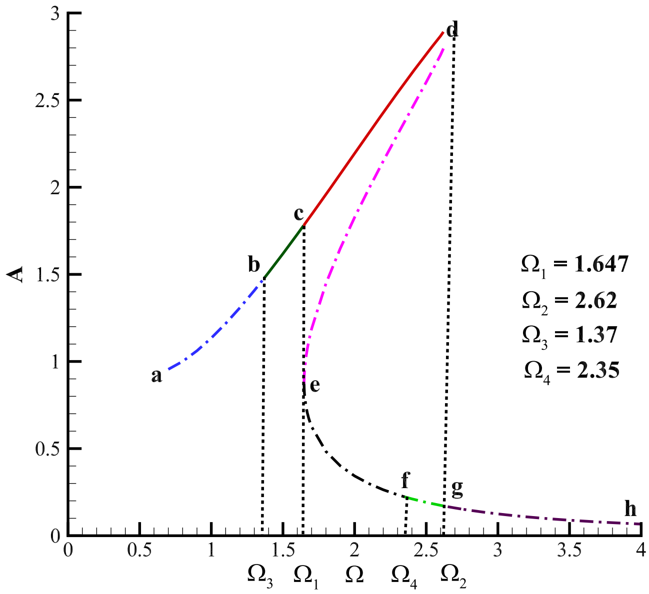


**Figure 3.** The frequency-response curve in the case of $\mu = \frac{1}{10}$, $\Omega_0 = \alpha = F = 1$.

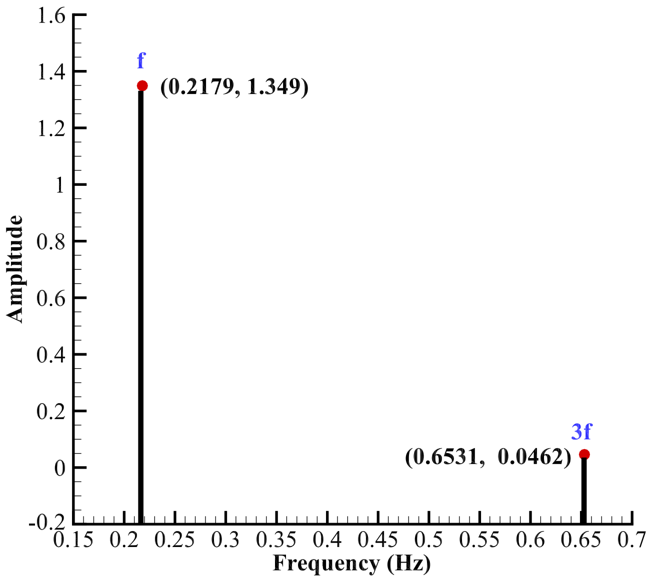


**Figure 4.** The frequency spectrum in the case of $\mu = \frac{1}{10}$, $\Omega_0 = \alpha = F = 1$, $\Omega = \frac{137}{100}\left(f = \frac{\Omega}{2\pi} = 0.218042\right)$.

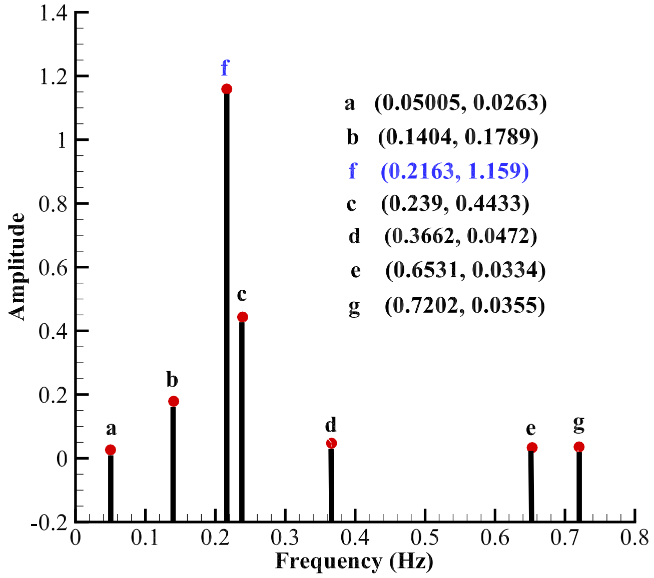


**Figure 5.** The frequency spectrum in the case of $\mu = \frac{1}{10}$, $\Omega_0 = \alpha = F = 1$, $\Omega = \frac{136}{100}\left(f = \frac{\Omega}{2\pi} = 0.216451\right)$.

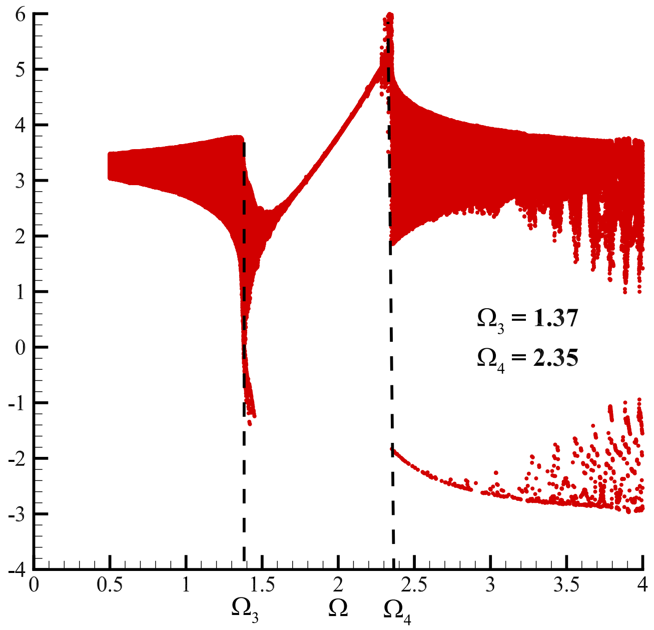


**Figure 6.** The bifurcation diagram in the case of $\mu = \frac{1}{10}$, $\Omega_0 = \alpha = F = 1$.

(1) The stable/unstable periodic series solutions of the Van der Pol–Duffing forced oscillator are obtained by the HAM, but numerical methods such as the fourth-order Runge Kutta are invalid for the unstable periodic solutions. The stability of the periodic solutions obtained is analyzed in the context of Floquet theory.

(2) Meanwhile, spectral analysis and bifurcation theory also support the above analyses.

(3) Two branches of the frequency-response curve of the Van der Pol–Duffing forced oscillator are unstable, which is different from the general conclusion that only one branch of the frequency-response curve of the Duffing forced oscillator is unstable with the same parameters. As such, the jump phenomena can be observed from the Duffing forced oscillator, however, it cannot be observed from the Van der Pol–Duffing forced oscillator.

In short, from what we understand, this paper pointed out three innovative points: first, the unstable periodic solutions of the Van der Pol–Duffing forced oscillator can be obtained analytically using HAM, but numerical methods such as the fourth-order Runge Kutta cannot; second, the stability of the periodic solutions obtained is analyzed in the light of Floquet theory; third, the jump phenomena cannot be observed from the Van der Pol–Duffing forced oscillator based on a set of parameters, which is different from the Duffing forced oscillator.

## Appendix: stability analysis

To ascertain the stability of the periodic solution, Floquet theory is applied. Considering the infinitesimal disturbance $\epsilon(t)$, the periodic solution is in the form

$$\bar{x}(t) = x(t) + \epsilon(t) \tag{29}$$

Substituting $\bar{x}(t)$ into equation (1) and keeping only linear terms of $\epsilon(t)$, it follows that

$$\ddot{\epsilon} - \mu\left(1 - x^2\right)\dot{\epsilon} + \left(2\mu x\dot{x} + \Omega_0^2 + 3\alpha x^2\right)\epsilon = 0 \tag{30}$$

which is a linear ordinary differential equation with periodic coefficients. Due to

$$x(t + T) = x(t) \tag{31}$$

equation (30) is periodic with period $T$. There exist two linearly independent solutions $\epsilon_1(t)$and$\epsilon_2(t)$, and the fundamental matrix solution of equation (30) is given by

$$\Phi(t) = \begin{pmatrix} \epsilon_1(t) & \epsilon_2(t) \\ \dot{\epsilon}_1(t) & \dot{\epsilon}_2(t) \end{pmatrix} \tag{32}$$

which satisfies

$$\Phi(t + T) = C\Phi(t) \tag{33}$$

where $C$ is a monodromy matrix associated with the fundamental matrix solution $\Phi(t)$.

Introducing $\Psi(t) = \begin{pmatrix} \xi_1(t) & \xi_2(t) \\ \dot{\xi}_1(t) & \dot{\xi}_2(t) \end{pmatrix}$, there exists

$$\Phi(t) = P \cdot \Psi(t) \tag{34}$$

where $P$ is a constant non-singular matrix. Substituting equation (34) into equation (33), we get

$$\Psi(t + T) = P^{-1}CP\Psi(t) = B\Psi(t) \tag{35}$$

where $B$ is a diagonal matrix of the form $B = \begin{pmatrix} \lambda_1 & 0 \\ 0 & \lambda_2 \end{pmatrix}$ and $B$and $C$ are similar matrices. Thus,

$$\xi_1(t + T) = \lambda_1\xi_1(t), \quad \xi_2(t + T) = \lambda_2\xi_2(t) \tag{36}$$

It follows from equation (36) that

$$\xi_1(t+nT) = \lambda_1^n \xi_1(t), \quad \xi_2(t+nT) = \lambda_2^n \xi_2(t) \tag{37}$$

where $n$ is an integer. Consequently, as time evolves $(n \to \infty)$

$$\xi_i \to \begin{cases} 0, & if\ |\lambda_i| < 1, \\ \infty, & if\ |\lambda_i| > 1. \end{cases} \tag{38}$$

and the disturbance $\epsilon(t)$ becomes unbounded with time if the modulus of any eigenvalue is larger than 1.

## Acknowledgments

We would like to express our sincere thanks to Professor Shijun Liao and Professor Liqun Chen for their helpful and enlightening discussions. We are grateful to the NSFC (Approval No.11272209 and No.51209136), and National Key Basic Research Program of China (Approval No.2014CB046801) for financial support.

## References

[1] Kahn P B and Zarmi Y 2004 Weakly nonlinear oscillations: a perturbative approach *Am. J. Phys* **72** 538–52
[2] Ueda Y and Akamatsu N 1981 Chaotically transitional phenomena in the forced negative-resistance oscillator *IEEE Trans. Circuits Syst.* **28** 217–23
[3] Kovacic I and Brennan M J 2011 *The Duffing Equation: Nonlinear Oscillators and Their Behaviour* (New York: Wiley)
[4] FitzHugh R 1961 Impulses and physiological states in theoretical models of nerve membranes *Biophysics. J* **1** 445–66
[5] Cartwright J and Eguiluz V 1999 Dynamics of elastic excitable media *Int. J. Bifurcation Chaos Appl. Sci. Eng.* **9** 2197–202
[6] Nayfeh A H and Mook D T 1979 *Nonlinear Oscillations* (New York: Wiley)
[7] Kao Y H and Wang C S 1993 Analog study of bifurcation structures in a Van der Pol oscillator with a nonlinear restoring force *Phys. Rev.* E **48** 2514–20
[8] Ghorbaniana P, Ramakrishnana S, Whitmanb A and Ashrafiuona H 2015 A phenomenological model of EEG based on the dynamics of a stochastic Duffing–Van der Pol oscillator network *Biomed. Signal Process Control* **15** 1–0
[9] Murali K and Lakshmanan M 1993 Transmission of signals by synchronization in a chaotic Van der Pol–Duffing oscillator *Phys. Rev.* E **48** 1624–6
[10] Shukla A K, Ramamohan T R and Srinivas S 2013 Analytical solutions for limit cycles of the forced Van der Pol–Duffing oscillator *AIP Conf. Proc* 1558 2187–92
[11] Stupnicka W S and Rudowski J 1994 Neimark bifurcation, almost-periodicity and chaos in the forced Van der Pol–Duffing system in the neighbourhood of the principal resonance *Phys. Lett.* A **192** 201–6
[12] Venkatesan A and Lakshmanan M 1997 Bifurcation and chaos in the double-well Duffing–Van der Pol oscillator: numerical and analytical studies *Phys. Rev.* E **56** 6321–30
[13] Chudzik A, Perlikowski P, Stefanski A and Kapitaniak T 2011 Multistability and rare attractors in Van der Pol–Duffing oscillator *Int. J. Bifurcation Chaos* **21** 1907–12
[14] Chen Y M and Liu J K 2009 Uniformly valid solution of limit cycle of the Duffing–Van der Pol equation *Mech. Res. Commun.* **36** 845–50
[15] Shukla A K, Ramamohan T R and Srinivas S 2014 A new analytical approach for limit cycles and quasi-periodic solutions of nonlinear oscillators: the example of the forced Van der Pol–Duffing oscillator *Phys. Scr.* **89** 10
[16] Steeb W H and Kunick A 1987 Chaos in limit cycle systems with external periodic excitations *Int. J. Non-Linear Mech.* **22** 349–61
[17] Liao S J 1992 Proposed homotopy analysis techniques for the solution of nonlinear problem *PhD Thesis* Shanghai Jiao Tong University
[18] Liao S J 2011 *Homotopy Analysis Method in Nonlinear Differential Equations* (New York: Springer)
[19] Cui J F, Lin Z L and Zhao Y L 2015 Limit cycles of nonlinear oscillator equations with absolute value by means of the homotopy analysis method *Z. Naturforsch., A: Phys. Sci* **70** 193–202
[20] Cui J F, Liao S J and Lin Z L 2015 Sub-harmonic resonances of periodic parameter excited oscillators with the absolute value items *AIP Conf. Proc* **1648** 650002
[21] Liu Y P, Liao S J and Li Z B 2013 Symbolic computation of strongly nonlinear periodic oscillations *J. Symb. Comput.* **55** 72–95
[22] Abbasbandy S 2008 Solitary wave solutions to the Kuramoto-Sivashinsky equation by means of the homotopy analysis method *Nonlinear Dynam* **52** 35–40
[23] Allan F M 2009 Construction of analytic solution to chaotic dynamical systems using the homotopy analysis method *Chaos Soliton Fract.* **39** 1744–52
[24] Hayat T and Sajid M 2007 On analytic solution for thin film flow of a fourth grade fluid down a vertical cylinder *Phys. Lett.* A **361** 316–22
[25] Turkyilmazoglu M 2009 Purely analytic solutions of the compressible boundary layer flow due to a porous rotating disk with heat transfer *Phys. Fluids* **21** 106014
[26] Gorder R A V and Kuppalapalle V 2011 Convective heat transfer in a conducting fluid over a permeable stretching surface with suction and internal heat generation/absorption *Appl. Math Comput.* **217** 5810–21
[27] Liang S X and Jeffrey D J 2009 An efficient analytical approach for solving fourth order boundary value problems *Comput. Phys. Commun.* **180** 2034–40
[28] Zou K G and Nagarajaiah S 2015 An analytical method for analyzing symmetry-breaking bifurcation and period-doubling bifurcation *Commun. Nonlinear Sci. Numer. Simul* **22** 780–92
[29] Stupnicka W S and Rudowski J 1997 The coexistence of periodic, almost-periodic and chaotic attractors in the Van der Pol–Duffing oscillator *J. Sound Vib.* **199** 165–75